# CHAPTER 2: STRUCTURAL ANALYSIS OF THE COFFS HARBOUR BLOCK

## INTRODUCTION

Within the Coffs Harbour Block three "generations" of folds have been identified, two being expressed on the mesoscopic scale and the third being obvious only on the macroscopic scale. The two mesoscopic generations have been separated by means of overprinting relationships and by different orientations of their structural elements. Throughout most of the block the rocks show only a single mesoscopic deformation which has produced folds varying from open to almost isoclinal. There is an axial plane cleavage, particularly in the pelitic rocks, and at some localities it has been folded during a second deformation. This is confined to isolated outcrops and is not widespread in occurrence.

It has been convenient to consider each "generation" of folds as a separate episode of deformation, but it is likely that the two mesoscopic sets are the product of one single progressive deformation (see Ramsay 1967, p.520), and the same might be true also of the macroscopic "set".

## REDBANK RIVER BEDS

### Preamble

The Redbank River Beds are lithologically distinct from the Coffs Harbour Sequence and work by the writer (Korsch 1973) showed that they are also structurally distinct. Only a summary of that work is given here, but more details are given of the morphology of the mesoscopic folds.

Two styles of folding are distinguished. The first, produced by an intense period of deformation, is tight or often isoclinal, and has axial surfaces with an average orientation of 025/E/45 (Plate 2A-E). Fold axes define a girdle of orientation 032/E/50 (Korsch 1973, Figs. 1i and 1j). Two distinct maxima on a $\pi$ plot of bedding occur at 34 to 290 and 55 to 302 and are taken to represent the orientations of the limbs of the folds (Korsch 1973, Fig. 1g).

PLATE 2

Folds from the Redbank River Beds

A. Fold with angular hinge, produced by the first period of deformation, in bedded cherts. This style of folding is common in the Redbank River Beds.

B. Isoclinal folds with thickening of the hinge area similar to those illustrated in Figure 18H.

C. Mesoscopic fold with rounded hinge. Dip isogons, stack inflection surfaces and train inflection surfaces for this fold are illustrated in Figure 18C and D.

D. Mesoscopic fold produced by the first period of deformation. The axial surface for this fold is curved due to folding by the second period of deformation.

E. Well rounded hinge areas in a fold produced by the first period of folding.

F. Gentle flexuring, produced by the second period of folding, and occurring on the limb of an earlier fold.

All folds occur on the headland at the mouth of the Redbank River near Red Rock village (GR 6341 2851). In each case the hammer denotes the scale.

A

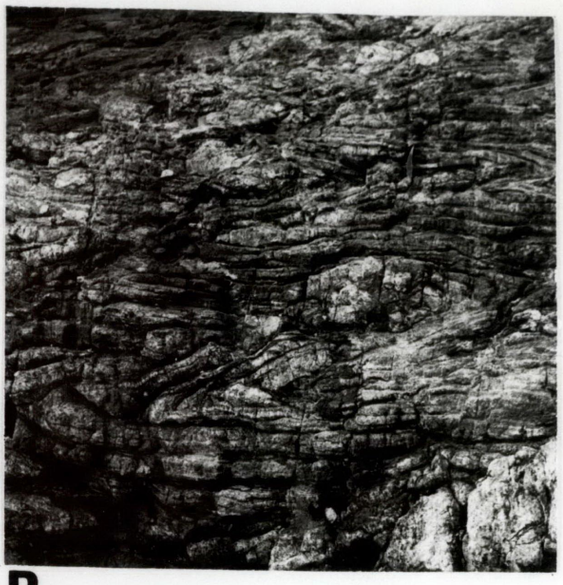

B

C

D

E

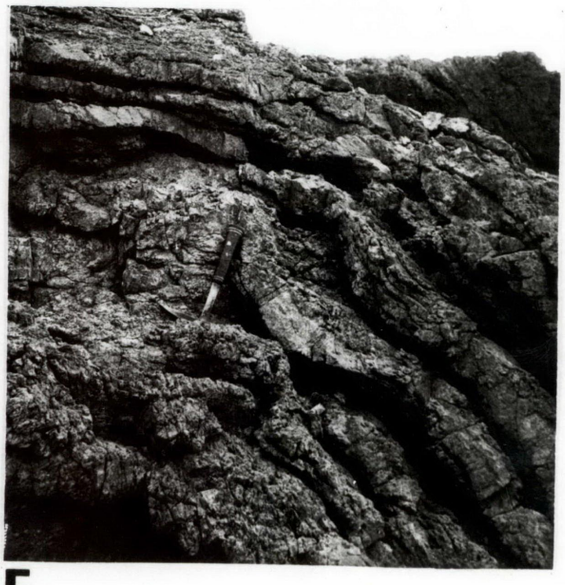

F

The second style consists of gentle flexures on the limbs of the tight folds (Plate 2F). Fold Axes and poles to axial planes fall along a girdle with an orientation of 026/E/33 approximately (Korsch 1973, Fig. 1j). The writer concluded that the tight to isoclinal folds formed first and were later affected by flexuring but the cause of the variable orientations of the axial planes of the flexures remains undetermined.

Morphology of the mesoscopic folds

The hinges of the tight folds show a progressive change in curvature and interlimb angle from rounded, through angular to almost true isoclinal (Fig. 18). Most folds are plane cylindrical with no cleavage and only very rare fractures in the hinge zone. They are generally symmetrical and hence formulae for symmetrical folds have been applied in the analysis of them. Other features of their geometry are more complex. The shape of the folded layers may change up and down a stack and layers are thinned frequently in limbs and thickened in hinge areas (Fig. 18C, E, H). In some folds the limbs also have different orthogonal thicknesses (Fig. 18H).

Even though there are variations in dimensions the ratios of wavelength and amplitude to total fold length ($^{\lambda}/_{L}$ and A/L, Table 2) remain relatively constant. They occupy very small fields when plotted against the interlimb angles (Fig. 19). The interlimb angles for eight folded surfaces (surfaces 1 - 8, Fig 18) are very consistent with a mean of 39.0°. Low values of C (= $^{c}/_{f}$, Table 2) indicate the folds tend towards angularity in the hinges. Although the folded surfaces vary in size they maintain a constant shape relative to each other. The percent shortening (V) ranges from 55 - 72% with a mean of 62%.

Dip isogons for several stacks of form surfaces converge and diverge and in restricted layers are approximately parallel (Fig. 18A, C, E). In one stack three adjacent layers show different isogon patterns (layers b, c, d of Fold C, Fig. 18). Graphs of T and t compared with $\measuredangle$ (Fig. 20) indicate that individual layers have the characteristics of more than one of the classes of Ramsay (1967, p.365). The individual layers, as well as the stacks, therefore have compound classifications but there is a tendency towards classes 1C and 3, with classes 1B and 2 subordinately represented. A general scheme of alternating convergent (1C) and divergent (3) layers or groups of layers is apparent and it is inferred that the final folds are the result of flattening of flexures initially produced by buckling. The tendency of profiles to change up and down a stack supports this conclusion.

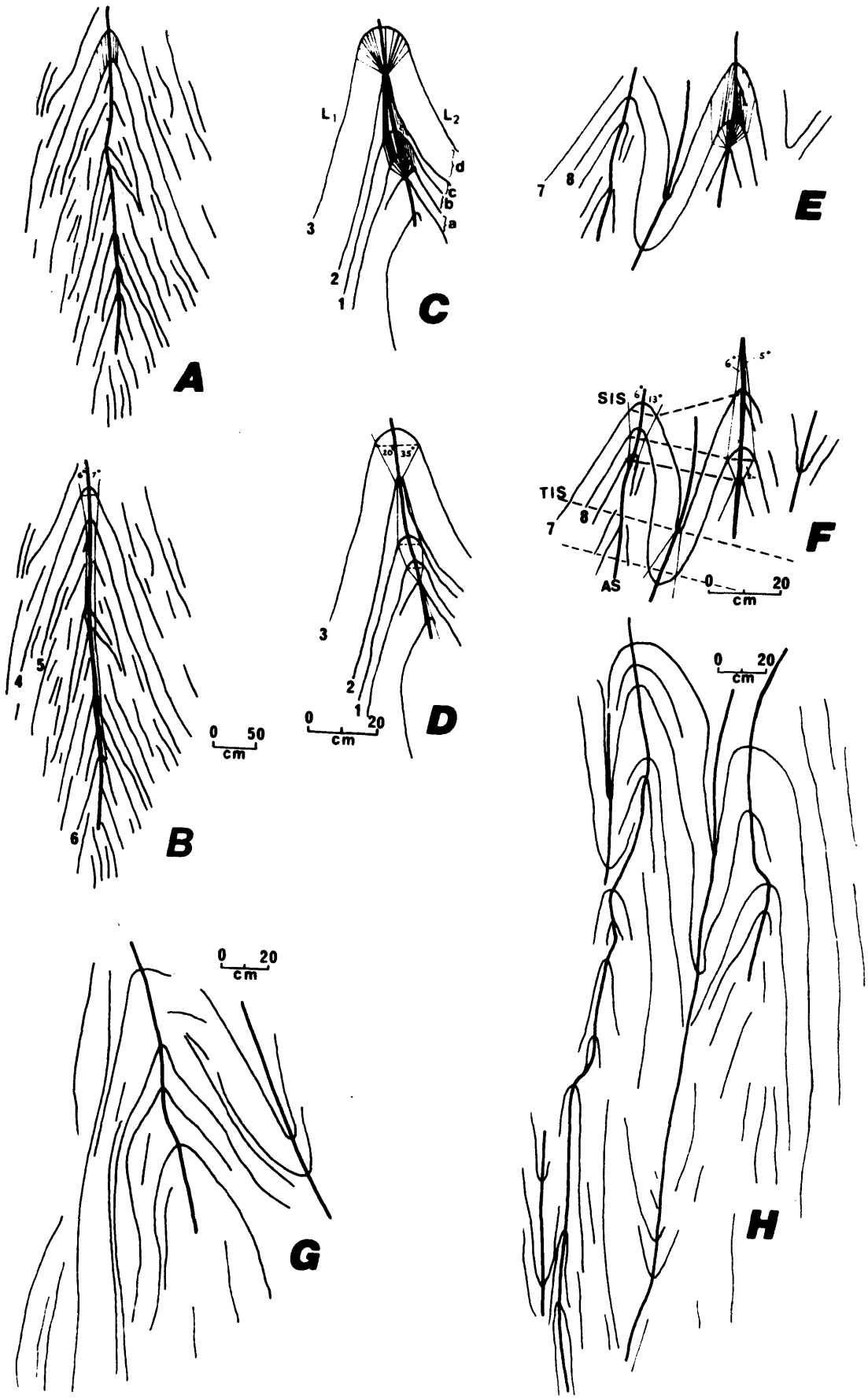


Fig. 18: Profile sketches of mesoscopic folds from the Redbank River Beds. Figs. A, C and E show dip isogon patterns and Figs. B, C and F show inflection surface traces. Figs. G and H show non planar axial surfaces.

Table 2: Dimensional data for mesoscopic folds from the Redbank River Beds
Values of c, f, $\lambda$, A and Z are given in metres, $\theta$ in degrees and V in percent

| Fold | Folded Surface | $\theta$ | c | f | $\lambda$ | A | V | c/f | $\lambda$/L | A/L | A/$\lambda$ | Z | Z/L |
|---|---|---|---|---|---|---|---|---|---|---|---|---|---|
| Fig. 18 | 1 | 40 | 0.07 | 0.75 | 0.59 | 0.33 | 61 | 0.09 | 0.39 | 0.22 | 0.57 | 0.31 | 0.21 |
| Fold C | 2 | 40 | 0.02 | 0.72 | 0.52 | 0.33 | 64 | 0.03 | 0.36 | 0.23 | 0.65 | 0.33 | 0.23 |
| | 3 | 42 | 0.13 | 0.75 | 0.67 | 0.32 | 55 | 0.17 | 0.45 | 0.21 | 0.47 | 0.27 | 0.18 |
| Fig. 18 | 4 | 41 | 0.18 | 2.80 | 2.15 | 1.25 | 59 | 0.06 | 0.41 | 0.22 | 0.58 | 1.21 | 0.22 |
| Fold B | 5 | 41 | 0.10 | 2.60 | 1.93 | 1.19 | 63 | 0.04 | 0.37 | 0.23 | 0.62 | 1.16 | 0.22 |
| | 6 | 32 | 0.08 | 2.60 | 1.48 | 1.23 | 72 | 0.03 | 0.28 | 0.23 | 0.83 | 1.15 | 0.22 |
| Fig. 18 | 7 | 40 | 0.03 | 0.44 | 0.33 | 0.20 | 62 | 0.08 | 0.38 | 0.22 | 0.60 | 0.19 | 0.21 |
| Fold E | 8 | 36 | 0.07 | 0.45 | 0.36 | 0.20 | 60 | 0.16 | 0.40 | 0.22 | 0.54 | 0.17 | 0.19 |
| | Mean | 39.0 | | | | | 62 | 0.08 | 0.38 | 0.22 | 0.61 | | 0.21 |

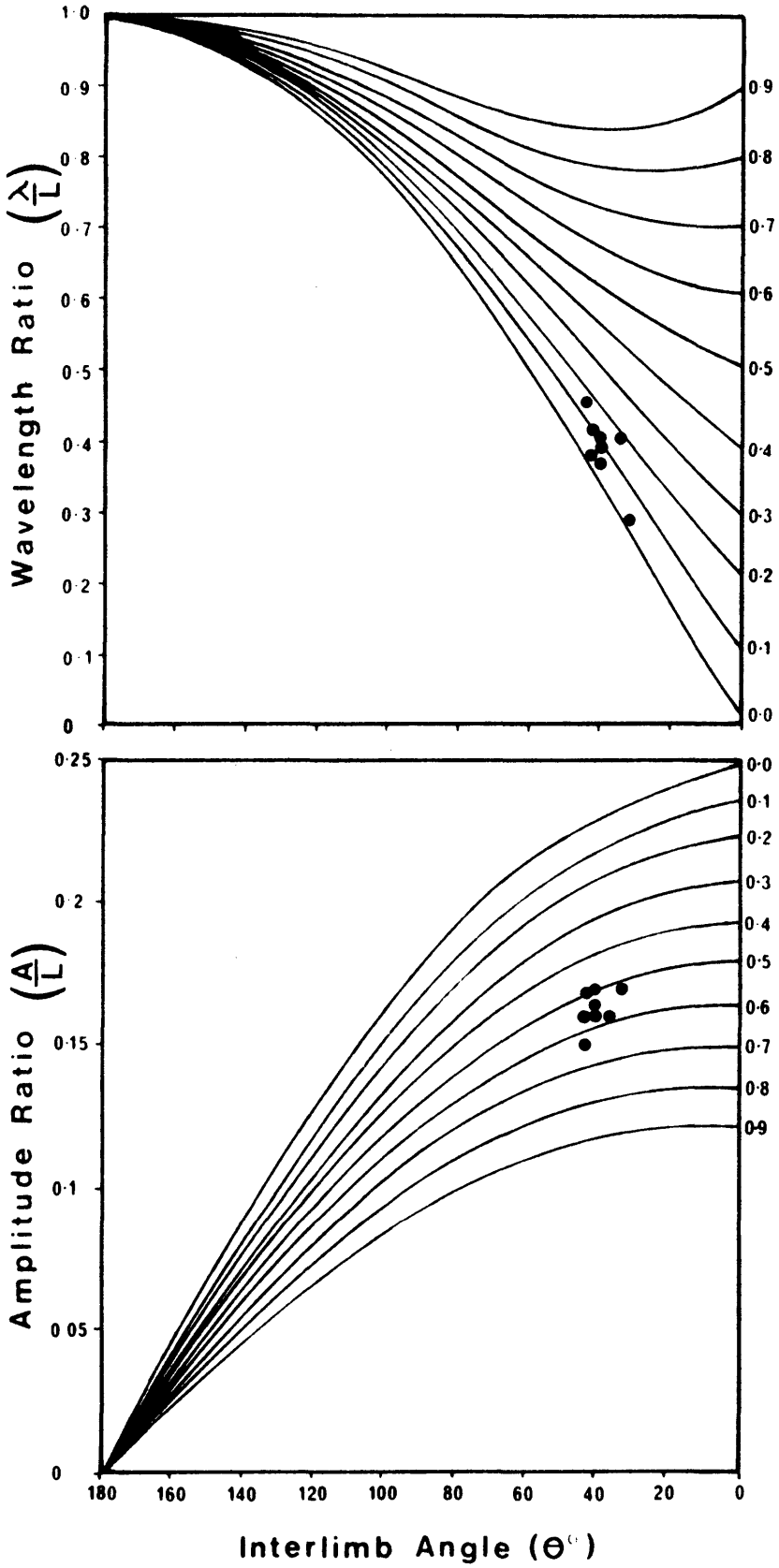


Fig. 19: $\frac{\lambda}{L}$ and $\frac{A}{L}$ versus $\theta$ curves showing positions of folded surfaces of folds from the Redbank River Beds.

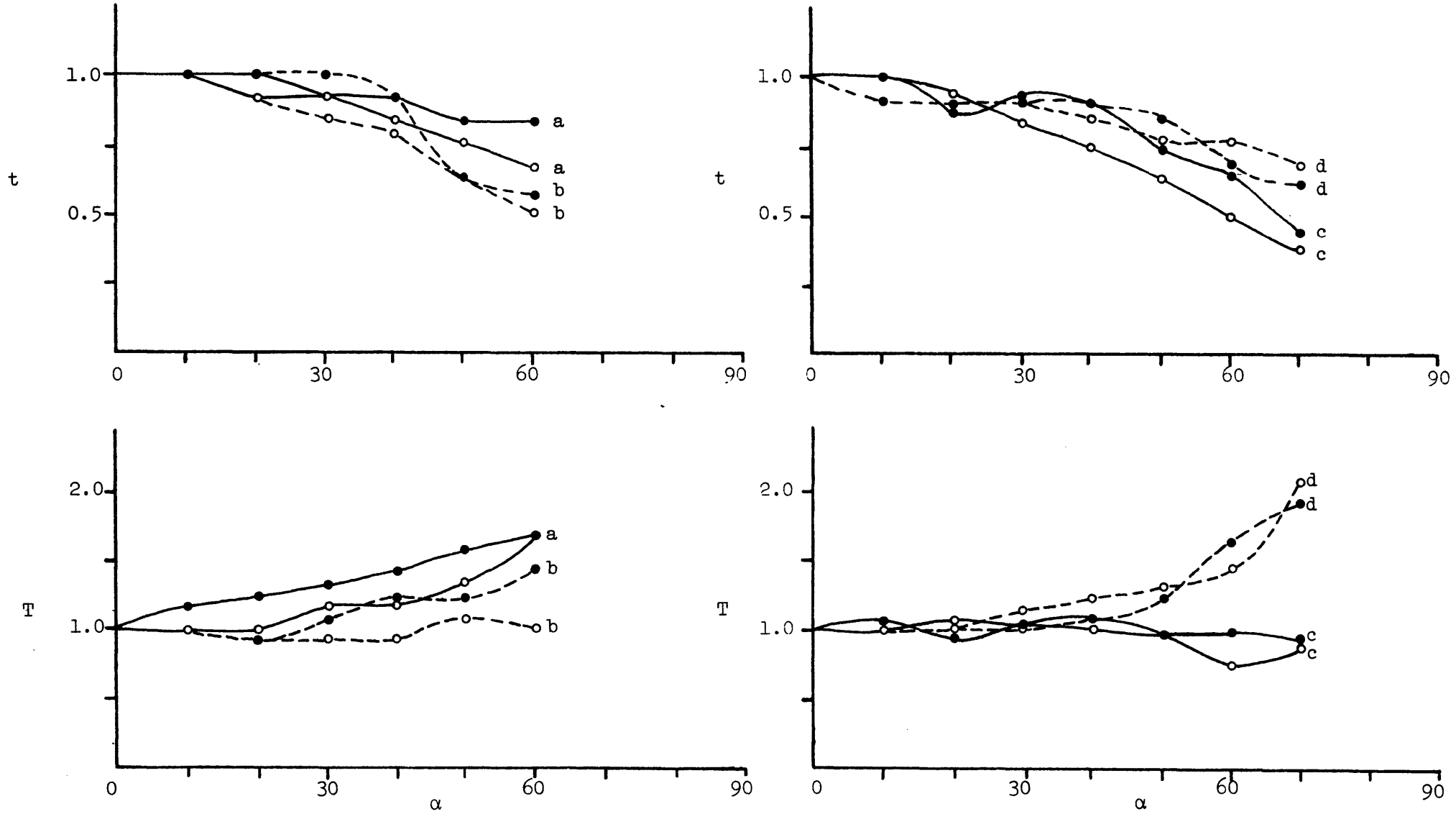


Fig. 20: Comparison of t and T with α for folds from the Redbank River Beds
• - Limb 1, o - Limb 2.

No uniform pattern emerges from the inflection surfaces for folds B, D and F (Fig. 18). In fold B the SIS is subparallel with AS and almost coincident with it, as in an idealised angular fold. Values for the ratio of the thickness of the zone of constant curvature to the total fold length (Z/L, Table 2) are remarkably uniform for the eight folded surfaces examined. The angles between SIS and AS ($\phi$) range from 5° to 35° for folds D and F but $\phi$ = 0° for fold B (Fig. 18). TIS is normal to AS or approximately so. The axial surface traces are non-linear, being slightly deformed by the later gentle flexuring. Because of the later slight alteration of the tight folds the patterns described here only equate approximately with the theoretical models described in Chapter 1.

## STRUCTURE OF THE COFFS HARBOUR SEQUENCE

### Mesoscopic Structures

#### PREDEFORMATIONAL STRUCTURES

Bedding is a prominent layering in the finer grained sediments and the bedding thicknesses are described in Appendix I (p.35). It is from these distinctly bedded units that most of the structural data have been recorded, because the very thick massive units (Korsch 1971, p.65) are devoid of primary marker surfaces.

Linear structures such as parallel flute and groove casts, and other primary linear structures, are rarely encountered and hence are of little practical value as structural markers. (This contrasts with the Rockvale Block where, at one locality, groove casts have been used as a primary lineation for structural analysis).

#### STRUCTURES PRODUCED BY THE FIRST DEFORMATION (D1)

1. Planar structures ($S_1$)

(a) Geometry

The earliest tectonic surface in the sediments is a fracture cleavage which near the southern boundary of the Block merges into slaty cleavage. The fracture cleavage is penetrative within an argillaceous layer but is not penetrative on the scale of an outcrop, being only weakly developed or non-existent in coarse-grained rocks. The slaty cleavage tends

to be more penetrative at outcrop scale than the fracture cleavage but is still less well developed in the coarse-grained rocks. Thin sections normal to the fracture cleavage show no preferred orientation of minerals and no visible neocrystallisation (as defined by Fairbain 1949) parallel to the cleavage surface. In some thin sections of slaty cleavage there is a strongly developed preferred orientation, particularly of white mica flakes (e.g. Appendix I, Plate 8C).

The spacing of the cleavage planes ranges from about 0.5 mm in the slaty cleavage to 2 - 5 mm in the fracture cleavage in fine-grained lithologies. The cleavage in coarse units is much more widely spaced.

Korsch (1973) has shown that the fracture cleavage in the Woolgoolga district is statistically parallel to the axial planes of the folds in the bedding (So) and this unusual relationship has now been found in D1 folds in So throughout the Block. In conformity with the statistical picture, there is little true fanning of the cleavage. However in the hinge zone of a few folds where there are alternating lithologies of differing anisotropism the cleavage does have marked deviations from the axial plane as in the theoretical pattern obtained by Dieterich (1969, Fig. 3) and in the fold illustrated by Siddans (1972, Fig. 18). It is stressed that fanning within a single bed is rare. On the other hand refraction of the cleavage between lithologies of differing grain-size and anisotropism is common, with angles of refraction changing up to 20° in passing from pelitic units to coarser units (Plate 7F).

Because the fracture cleavage and slaty cleavage are parallel they will be regarded as the same planar element ($S_1$ or FOLN 31) for the purposes of structural analysis.

One problem, discussed in Chapter 1 (p. 6 ), is the distinction between fracture and slaty cleavage. In an attempt to clarify this situation oriented hand specimens showing well developed cleavage planes were collected at several localities in the Block, and where possible their position in the form surface of a mesoscopic fold noted. On flat surfaces where the collection of a specimen was extremely difficult photographs were taken and later printed at a magnification x 1. Typical examples of the cleavage pattern are illustrated in Plates 3 to 6.

Work on the hand specimens also proved difficult until photographs of them were taken in the laboratory and printed on the same scale as the specimen. Traces of the photographs (e.g. Fig. 21) were analysed on an


Plate 3: Outcrop at south east corner of Arrawarra headland showing cleavage traces found typically in fine-grained lithologies from the Coramba Beds.

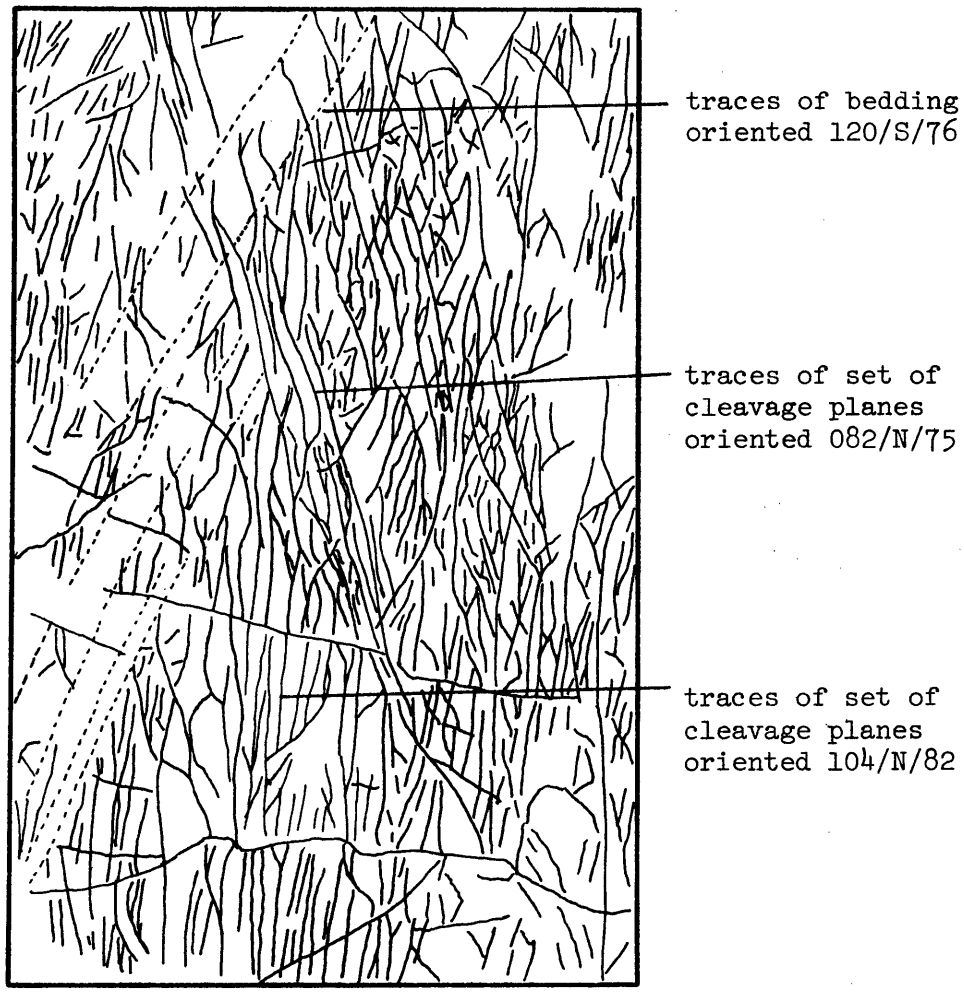


Plate 4: Two sets of cleavage traces intersecting a set of steeply dipping bedding planes. Traces were observed in a north-south striking subvertical joint plane located at the eastern end of Woolgoolga headland. Magnification of photograph x 1.

# PLATE 5

Patterns of Cleavage from the Coffs Harbour Block

A. Specimen A. Cleavage in mudstone from Unit D, Coramba Beds. Woolgoolga Headland, GR 6330 2695, magnification x 1.

B. Specimen 4. Cleavage in interbedded mudstone and fine-grained siltstone. The bedding planes can be seen near the top of the specimen, being cut at nearly right angles by the cleavage traces. Location same as Specimen A, magnification x 1.

C. Specimen 6. Cleavage in mudstone from Unit A, Coramba Beds. Mutton Bird Island, GR 6262 2458, magnification x 1.

D. Photograph 1-30B. Cleavage pattern in mudstone from Unit D, Coramba Beds showing a closely-spaced cleavage system being cut by a second more widely-spaced cleavage system. Arrawarra Headland, GR 6324 2756. Magnification x 1.

E. Photograph 1-30A. This photograph was taken from the same smooth surface as photograph 1-30B and the two photographs were taken approximately 1m apart. The second cleavage seen on photograph 1-30B is represented by only two planes on this photograph. Magnification x 1.

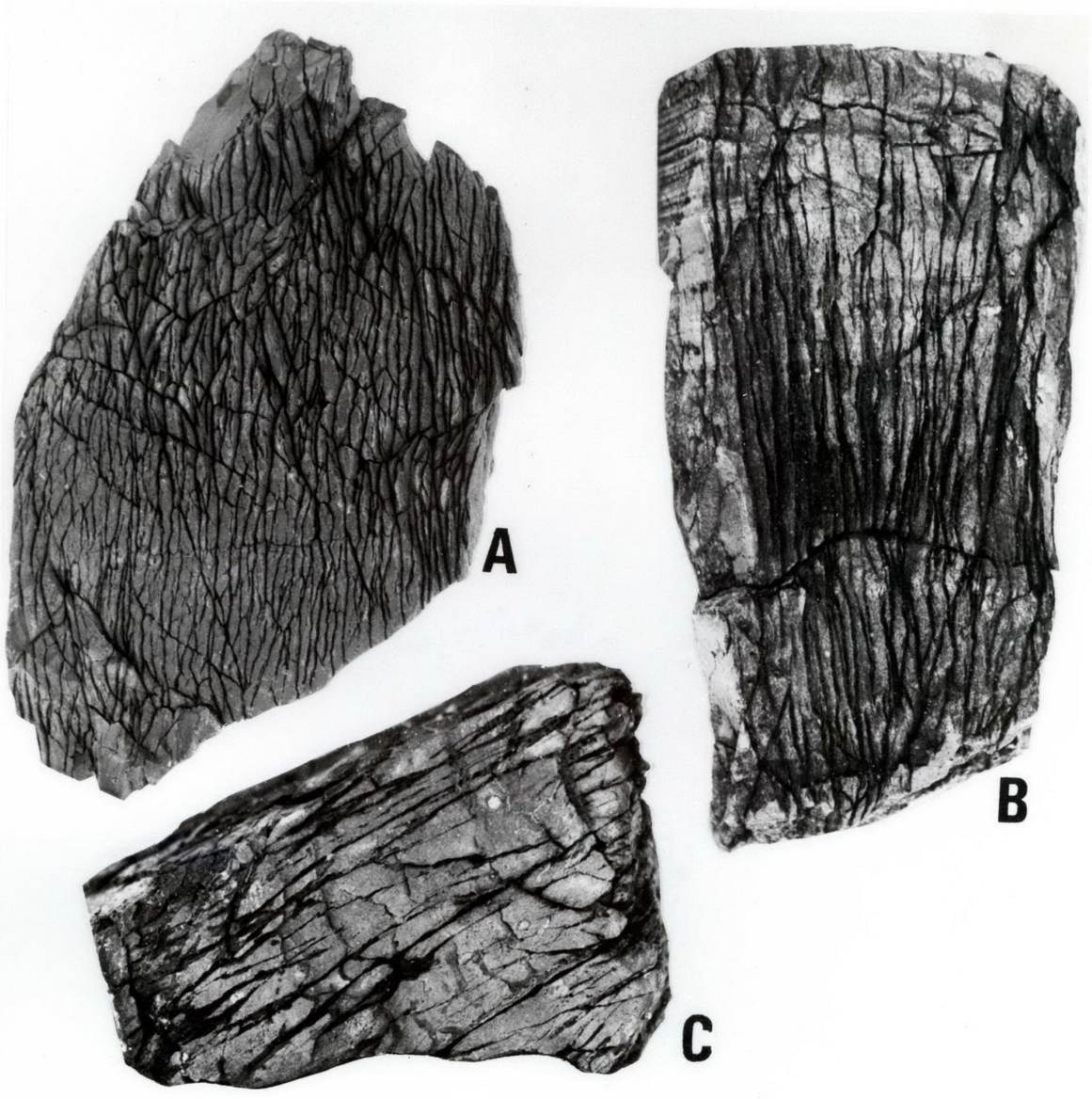
A
B
C


D


E

## PLATE 6

**Patterns of Cleavage from the Coffs Harbour Block**

A. Specimen 3A. Cleavage pattern in a mudstone from Unit D, Coramba Beds. Observed pattern is similar to that seen in Plate 5D (photograph 1-30B). Arrawarra Headland, GR 6324 2756, magnification x 3.

B. Specimen 2. Cleavage in a fine-grained siltstone. Same location as Specimen 3A. Magnification x 1.

C. Specimen 3B. This photograph was taken from the same hand specimen as Specimen 3A (Plate 6A). The planes illustrated are perpendicular to each other, with Specimen 3A occurring in the horizontal plane and Specimen 3B in the vertical plane. The top edge in this photograph joins the upper lefthand edge of Specimen 3A illustrated in Plate 6A. Magnification x 3.

D. Specimen 5. Cleavage pattern in a mudstone from Unit D, Coramba Beds. Woolgoolga Headland, GR 6330 2695, magnification x 1.

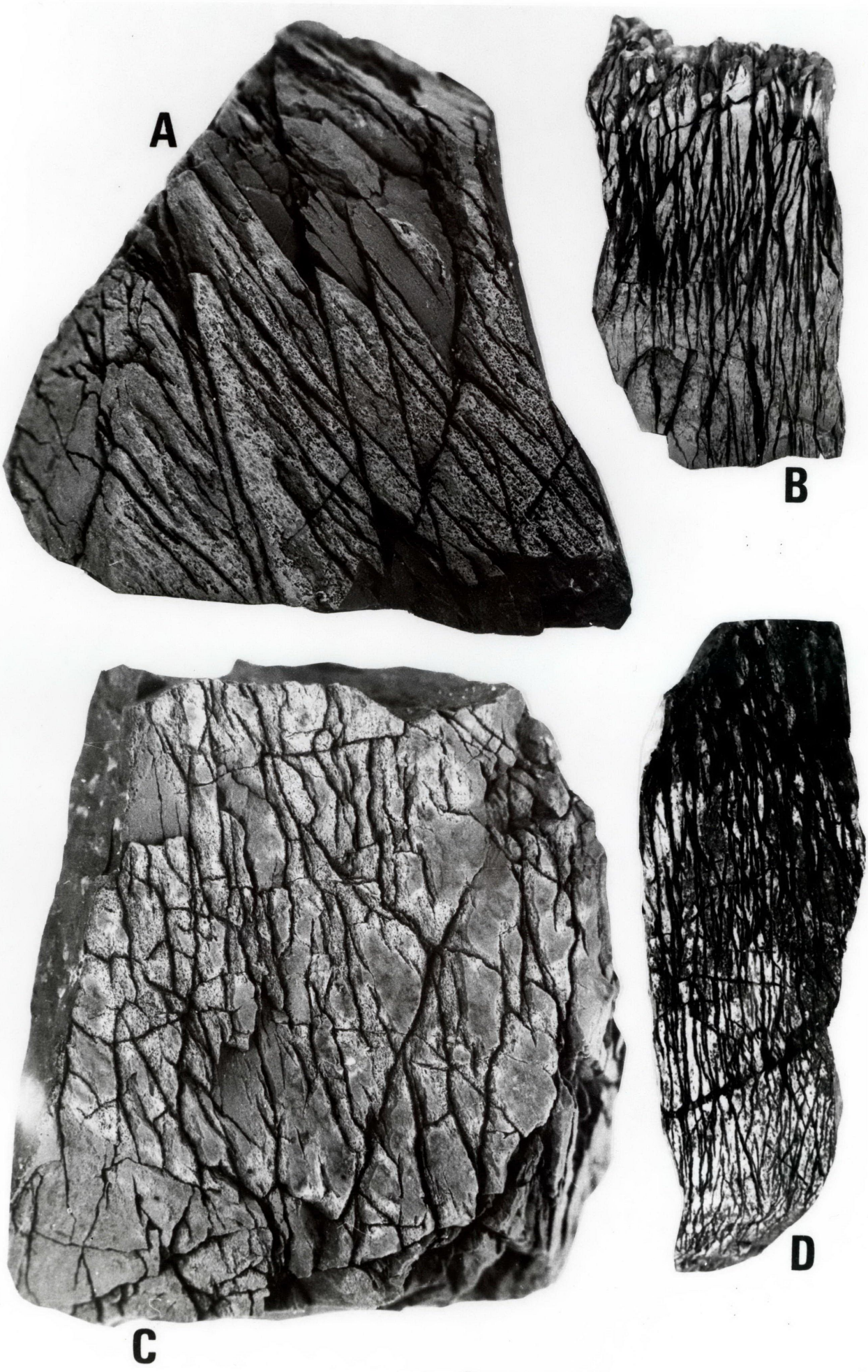
A
B
C
D